Kim *et al. Stem Cell Research & Therapy* (2024) 15:411
https://doi.org/10.1186/s13287-024-04020-8

Stem Cell Research & Therapy

RESEARCH Open Access

Post-symptomatic administration of hMSCs exerts therapeutic effects in SCA2 mice

Sehwan Kim[1,2†], Chanchal Sharma[1,3†], Jungwan Hong[2†], Jong-Heon Kim[2], Youngpyo Nam[2], Min Sung Kim[4], Tae Yong Lee[4], Kyung-Suk Kim[4], Kyoungho Suk[2,5], Ho-Won Lee[2,6] and Sang Ryong Kim[1,2*]

Abstract

Background Defects in the ataxin-2 (ATXN-2) protein and CAG trinucleotide repeat expansion in its coding gene, Atxn-2, cause the neurodegenerative disorder spinocerebellar ataxia type 2 (SCA2). While clinical studies suggest potential benefits of human-derived mesenchymal stem cells (hMSCs) for treating various ataxias, the exact mechanisms underlying their therapeutic effects and interaction with host tissue to stimulate neurotrophin expression remain unclear specifically in the context of SCA2.

Methods Human bone marrow-derived MSCs (hMSCs) were injected into the cisterna magna of 26-week-old wild-type and SCA2 mice. Mice were assessed for impaired motor coordination using the accelerating rotarod, open field test, and composite phenotype scoring. At 50 weeks, the cerebellum vermis was harvested for protein assessment and immunohistochemical analysis.

Results Significant loss of NeuN and calbindin was observed in 25-week-old SCA2 mice. However, after receiving multiple injections of hMSCs starting at 26 weeks of age, these mice exhibited a significant improvement in abnormal motor performance and a protective effect on Purkinje cells. This beneficial effect persisted until the mice reached 50 weeks of age, at which point they were sacrificed to study further mechanistic events triggered by the administration of hMSCs. Calbindin-positive cells in the Purkinje cell layer expressed bone-derived neurotrophic factor after hMSC administration, contributing to the protection of cerebellar neurons from cell death.

Conclusion In conclusion, repeated administration of hMSCs shows promise in alleviating SCA2 symptoms by preserving Purkinje cells, improving neurotrophic support, and reducing inflammation, ultimately leading to the preservation of locomotor function in SCA2 mice.

Keywords Spinocerebellar ataxia type 2, Mesenchymal stem cells, Purkinje cells, Neurotrophic factor, Follistatin-like 1, Neuroinflammation

[†]Sehwan Kim, Chanchal Sharma and Jungwan Hong have contributed equally to this work.

*Correspondence:
Sang Ryong Kim
srk75@knu.ac.kr
[1] School of Life Science and Biotechnology, BK21 FOUR KNU Creative BioResearch Group, Kyungpook National University, Daegu 41566, Korea
[2] Brain Science and Engineering Institute, Kyungpook National University, Daegu 41944, Korea
[3] Byrd Alzheimer's Centre and Research Institute, University of South Florida, Tampa, FL 33620, USA
[4] Bioengineering Institute, Corestemchemon Inc, Seoul 13486, Korea
[5] Department of Pharmacology and Biomedical Science, School of Medicine, Kyungpook National University, Daegu 41944, Korea
[6] Department of Neurology, Kyungpook National University Chilgok Hospital, Daegu 41404, Korea

© The Author(s) 2024. **Open Access** This article is licensed under a Creative Commons Attribution-NonCommercial-NoDerivatives 4.0 International License, which permits any non-commercial use, sharing, distribution and reproduction in any medium or format, as long as you give appropriate credit to the original author(s) and the source, provide a link to the Creative Commons licence, and indicate if you modified the licensed material. You do not have permission under this licence to share adapted material derived from this article or parts of it. The images or other third party material in this article are included in the article's Creative Commons licence, unless indicated otherwise in a credit line to the material. If material is not included in the article's Creative Commons licence and your intended use is not permitted by statutory regulation or exceeds the permitted use, you will need to obtain permission directly from the copyright holder. To view a copy of this licence, visit http://creativecommons.org/licenses/by-nc-nd/4.0/.

Introduction

Spinocerebellar ataxia type 2 (SCA2) is a progressive neurodegenerative disorder affecting the cerebellum and characterized by neuroinflammation, progressive incoordination (ataxia), and muscle weakness. It is the second most common subtype of autosomal dominant cerebellar ataxia (CA) worldwide, after SCA3, and remains an incurable disease despite being identified decades ago [1, 2]. Additionally, it is the most severe subtype among the 43 known SCA subtypes [2, 3], affecting motor coordination in the upper body more severely than that in the lower body [4, 5]. Clinically, individuals with SCA2 present with a progressive cerebellar syndrome characterized by a myriad of motor and non-motor impairments, including ataxia, dysarthria, dysphagia, oculomotor dysfunction, rigidity, bradykinesia, somatosensory deficits, executive dysfunction, and late cognitive decline [1, 3, 6]. Genotypically, the disease is caused by toxic "gain-of-function," which results in CAG trinucleotide repeat expansion, thus crossing a certain threshold in the coding region of the ataxin-2 (*Atxn-2*) gene, which maps to 12q23-q24.1 [2, 3]. The *Atxn-2* gene typically contains approximately 22 CAG repeats. Variations of up to 31 repeats are considered nonpathogenic and do not present harmful phenotypic effects [2, 7]. However, the number of repeats can influence disease severity and symptom onset age [2, 3]. For instance, individuals with ≥ 33 CAG repeats in the *Atxn-2* gene tend to develop signs and symptoms of SCA2. People with 33–34 repeats are more likely to exhibit signs and symptoms of SCA2 in late adulthood, whereas those with >45 repeats are more likely to display symptoms in their teens [3]. Further, this polyglutamine expansion in the protein ataxin-2 affects motor coordination owing to cellular death across several brain regions, especially in the cerebellar cortex, pontine nuclei, inferior olives, and peripheral nerves, thus often resulting in premature death [1–3, 6, 8].

In terms of current therapeutic options for SCA2, stem cell-based therapies hold great promise owing to their multi-lineage development, immunomodulatory activities, and trophic properties [9, 10]. Furthermore, in comparison to other types of stem cells, human bone marrow-derived mesenchymal stem cells (hMSCs) provide several advantages, including their widespread availability, the minimal ethical concerns over their use, and the ability to be isolated from various organs and tissues [11, 12]. This broad availability paves the way for their application in human clinical trials, thus opening avenues for their therapeutic application in neurodegenerative diseases, such as SCA2 [9, 11, 13, 14]. Additionally, clinical studies conducted on SCA3 patients and SCA2 transgenic animals have demonstrated that hMSC infusion may partially restore motor function in both clinical and preclinical trials [15, 16]. We also recently reported that hMSC treatment not only inhibited the symptoms of neuroinflammation in a lipopolysaccharide (LPS)-induced CA mouse model but also modulated microglial M2 polarization via increased tumor necrosis factor-stimulated gene-6 (TSG-6) levels and inhibited apoptosis [17]. Additionally, multiple administrations of hMSCs protected Purkinje and cerebellar granule cells by stimulating neurotrophic factors and inhibiting cerebellar inflammatory responses, thereby improving motor behavior, in a cytosine β-D-arabinofuranoside hydrochloride (Ara-C)-induced CA mouse model [18]. Overall, hMSCs are an ideal candidate cell type for tissue engineering and regenerative medicine [9], though the precise mechanisms by which they interact with host tissue to stimulate the expression of neurotrophins and suppress neuroinflammation are not yet fully understood.

Follistatin-like protein 1 (FSTL1) is a transforming growth factor (TGF)-β1-inducible glycoprotein belonging to the "secreted protein acidic and rich in cysteine" family of matricellular proteins found in MSCs with an unclear function [19–21]. Earlier reports suggest FSTL1 is an immune modulator, and it has been shown to modify cell growth, cell survival, cell proliferation, cell differentiation, tissue repair and alteration, inflammation, and embryogenesis and [20, 22]. FSTL1 can regulate MSC proliferation and chondrogenic differentiation, crucial processes for tissue healing [21]. Furthermore, FSTL1-overexpressing MSCs have been found to reduce inflammatory cell infiltration and increase lifespan against hypoxia in vivo [23]. Additionally, FSTL1 has been reported to enhance the pro-survival effects of bone-derived neurotrophic factor (BDNF) on neurons [24], and helps to promote cell survival and inhibit apoptosis both in vitro and in vivo [24–30]. In our recent study, we reported the downregulation of FSTL1 in the secretome of CA MSCs, which coincided with the suppression of proinflammatory microglial activation [31]. While the role of FSTL1 in inflammation is still debated, a few reports suggest FSTL1 suppresses inflammatory activation of microglia and astrocytes both in vitro and in vivo, and can downregulate the expression of cytokines such as tumor necrosis factor-alpha (TNF-α), interleukin-1 beta (IL-1β), and interleukin-6 (IL-6), which are known to contribute to neuroinflammation [22].

While the underlying cause of SCA2 is a repeat expansion in the *ATXN2* gene [1, 6], emerging research suggests that the loss of neurotrophic support and neuroinflammation may also contribute to disease progression [32, 33]. Therefore, the neuroprotective properties of FSTL1 make it an intriguing candidate for therapeutic interventions in SCA2. In this study, our aim was to investigate the potential neurotrophic and anti-inflammatory effects

of multiple hMSC administrations in an SCA2 transgenic mouse model, shedding light on the potential role of FSTL1 as a determinant of the neuroprotective effects mediated by hMSCs.

Methods

Animals

Wild-type (WT) male C57BL/6 J mice (aged 8 weeks and weighing approximately 20–25 g) were obtained from Daehan Biolink (Eumseong, Korea). To address the challenges associated with accurately identifying the onset of SCA2, we used a transgenic mouse model that expressed full-length *Atxn-2*-complementary DNA under the control of the Purkinje cell protein-2 promoter, which specifically targets Purkinje cells [34, 35]. Both male and female SCA2 mice were purchased from Jackson Laboratories and were genotyped in a controlled environment. SCA2 genotype was confirmed by polymerase chain reaction (PCR) using a 5′-AATACCTATGACGCCCATGC-3′ (transgene forward), 5′-ATGAGCCCCGTACTGAGTTG-3′ (transgene reverse), 5′-CTAGGCCACAGAATTGAAAGATCT-3′ (internal positive control forward) and 5′-GTAGGTGGAAATTCTAGCATCATCC-3′ (internal positive control reverse) primer sets designed to distinguish expansion-positive samples (transgene- 346 bp) from those without a repeat expansion (Supplementary Fig. 1A). The PCR product was separated by electrophoresis in a 1.5% agarose gel, stained with RedSafe nucleic acid stain, and visualized under ultraviolet light. Further, the presence of ATXN-2 protein was also confirmed in the cerebellum of the SCA2 mice model in an age-dependent manner using immunoblot analysis (Supplementary Fig. 1B,C).

The mice were housed in a controlled environment (12 h light/12 h dark conditions) with ad libitum access to water and food. All behavioral and protein-based experiments were conducted using a sample size of n = 6. The experimental animals were treated humanely. The animal experiments in this study adhered to the ARRIVE guidelines (Supplementary file 2), and all animal protocols were approved by the Animal Care Committee of Kyungpook National University [Approval numbers and dates: KNU 2023-0140 and 2024-0095 (Approved project title: Development of new therapeutics to overcome neurodegenerative diseases), with approvals obtained on May 9, 2023, and Feb 27, 2024, respectively].

hMSC preparation and injection

The study was conducted under the project namely, "Study on therapeutic validation and mechanism of mesenchymal stem cell in animal model of cerebellar ataxia", granted and funded by Korea Health Industry Development Institute (Grant No. HI16C2210). The hMSCs were obtained from the bone marrows of eight healthy individuals according to the reviewed and approved protocols of the Institutional Review Board (IRB) of Kyungpook National University Chilgok Hospital (IRB: 2019-02-008-002). All the participants and their caregivers provided written informed consent for participation in this study.

The MSCs used in the experiments were not pooled, and throughout all experiments, MSCs from a single donor were used for each test. The selection of this donor's MSCs was based on their superior initial proliferative capacity, which allowed for the prioritization of banked MSCs with a higher cell count. The MSCs utilized in the experiments were at Passage 3 or 4. The culturing followed the same methods as in previous study [36], including tests for morphology, surface markers, and differentiation potential, using passage 3 or 4 cells for the experiments. Isolated hMSCs were characterized and expanded under "Good Manufacturing Practice" conditions at CorestemChemon Inc. (Seoul, Korea), according to the International Society of Cellular Therapy guidelines [36]. Briefly, cells were seeded at a density of 11.5×10^7 cells/cm^2 and cultured in CSBM-A06 medium (CorestemChemon Inc., Seoul, Republic of Korea) supplemented with 10% fetal bovine serum (Life Technologies-Thermo Fisher Scientific, Waltham, MA, USA), 2.5 mM L-alanyl-L-glutamine (Merck Biochrom AG, Berlin, Germany), and 1% penicillin–streptomycin (Merck Biochrom AG, Berlin, Germany). To ensure cell purity, nonadherent and dead cells were removed through washing, and the medium was replaced twice a week. Passage 0 (P0) cells were defined as adherent cells that reached 70%–80% confluence. At passage 3 or 4 (P3 or P4), the cells were analyzed using flow cytometry to determine their cell surface marker expression. hMSCs were characterized as CD29/CD44/CD73/CD105-positive and CD34/CD45-negative cells [17, 18].

Studying mice at 25 weeks of age generally corresponds to a stage in disease progression that mirrors the symptom onset observed in human patients with SCA2. This stage is characterized by the degeneration of Purkinje cells and development of motor abnormalities [37–42]. Therefore, hMSCs were injected into 26-week-old SCA2 mice via both single injection (SI) and multiple injection (MI), followed by double the administration of hMSCs via MI every 4 weeks till the mice had reached 34 weeks of age (Fig. 1A). Further, both WT and SCA2 mice were subjected to behavioral tests assessing different motor abilities (rotarod, open-field, ledge, hindlimb clasp, and gait testing) at 4-week intervals from 26 to 50 weeks of age. At the end of the study, mouse brains were extracted for western blot and immunohistochemical analyses (Fig. 1A). The mice were randomly divided into nine experimental

groups (1) WT-intact, (2) WT-HypoThermosol™ (HTS), (3) WT-hMSC-1×10^5: MI, (4) SCA2-intact, (5) SCA2-HTS, (6) SCA2-hMSC-6×10^4: SI, (7) SCA2-hMSC-6×10^4: MI, (8) SCA2-hMSC-1×10^5: SI and (9) SCA2-hMSC-1×10^5: MI. For anesthesia, mice were injected intraperitoneally with a mixture of ketamine, chemically known as 2-(2-chlorophenyl)-2-(methylamino) cyclohexanone hydrochloride (115 mg/kg, Yuhan Corporation, Seoul, Korea, Cat. No. 8806421050721) and Rompun, composed of xylazine hydrochloride and methyl hydroxybenzoate (23 mg/kg, Bayer Korea Ltd., Seoul, Korea, Cat. No. 86140632–01) [13]. Following the administration of the ketamine/xylazine mixture, their anesthesia status was confirmed before proceeding with the hMSC injection. For multiple hMSC injections, 26-week-old mice received three injections at 4-week intervals, with their condition monitored and hMSCs administered before each procedure. The mice were also treated with HTS, an optimized preservation medium used to maintain stem cells at low temperatures and mitigate temperature-induced molecular cell stress responses, and it was used as a control for hMSC administration [17, 18]. The head of the mouse was positioned at an angle of approximately 90° to the body in a stereotaxic frame. After exposing the dura mater by pushing the muscle layers using forceps, hMSCs (6×10^4 cells/20 μL or 1×10^5 cells/20 μL) were injected into the cisterna magna using a Hamilton syringe (25 μL, 30-gauge) attached to a syringe pump (2 μL/min) (Fig. 1A). The needle was removed 10 min later and the incision closed with a silk suture. Seven days after hMSC injection, the silk suture was removed, and the mice were treated with povidone–iodine to treat their scars and reduce the risk of infection. Since the mice had undergone three hMSC injections, this process was repeated after each surgery.

Behavioral tests

Motor coordination, strength, and balance were assessed using a rotarod apparatus as described previously with some modifications [17, 18, 43, 44]. Briefly, all mice underwent acclimation training. This training consisted of three pretrials per day for three days, with each trial lasting 10 min at a speed of 10 rpm to minimize stress and ensure baseline performance. Mice were placed on a rotarod with a diameter of 3 cm. The speed of the rotarod was gradually increased from 4 to 40 rpm over a span of 5 min and then maintained at 40 rpm for an additional 5 min, making each trial 10 min in total. The test experiments began when WT and SCA2 mice were 26 weeks of age and were repeated at 4-week intervals until they reached 50 weeks of age. To prevent muscle fatigue, each mouse had a 1 h rest interval between trials. Latency to fall was recorded and averaged across 3 trials per session (n = 6 mouse/group).

The open-field test was conducted once after 4 weeks of hMSC transplantation, in 26-week-old mice, with some modifications [18]. Each mouse was placed individually in a white acrylic box arena measuring 40 × 40 × 40 cm. Their behavior was recorded for 4 min using a video recording system, and the recorded data were analyzed using the SMART 3.0 video-tracking software (Panlab-SMART). To ensure cleanliness, the arena was wiped with 70% ethanol between tests. The tests were carried out in a low luminous intensity environment to minimize stress and optimize the accuracy of the assessment of locomotor activity.

To assess the effects of hMSC administration, a composite phenotype scoring system consisting of a ledge test, hindlimb clasping test, and gait test was utilized. The tests were conducted once every 4 weeks, while mice were 26–50 weeks old, following previously established protocols [45, 46]. All tests were graded on a scale ranging from 0 to 3, where a score of 0 denoted the absence of the specific phenotype, and a score of 3 represented the

(See figure on next page.)

Fig. 1 Beneficial effects of human mesenchymal stem cells (hMSCs) on behavioral impairment and neuronal damage in spinocerebellar ataxia 2 (SCA2) mice. **A** Experiment schematic of hMSC treatment in wild-type (WT) and SCA2 mice. The figure was created using Biorender.com (Agreement number: XL26IE3A0R). hMSC treatment was administered once (single injection; SI) or thrice (multiple injections; MI) at 4-week intervals in 26-week-old WT and SCA2 mice. **B**, **C** Western blot analysis of neuronal nuclear protein (NeuN) and calbindin in the cerebellum after 24 weeks of hMSC treatment (50-week-old mice). $^{**}p<0.01$ and $^{***}p<0.001$ *vs*. untreated WT mice; $^{\#}p<0.05$ and $^{\#\#\#}p<0.001$ *vs*. treated SCA2 mice (two-way analysis of variance [ANOVA] with Tukey's post-hoc analysis; n = 6 for each group). Full-length blots are presented in Supplementary Fig. 1 and Fig. 1B. **D** A behavioral test for motor coordination impairment was performed using the rotarod test in WT and SCA2 mice treated with hMSCs at 4-week intervals from 26 to 50 weeks of age. $^{***}p<0.001$ vs. untreated WT mice; $^{\#\#\#}p<0.001$ vs. untreated SCA2 mice (one-way ANOVA with Tukey's post hoc analysis; n = 6 for each group). **E** A behavioral test for locomotor activity was performed using the open-field test in WT and SCA2 mice at 4-week intervals after hMSC treatment. $^{*}p<0.05$ vs. untreated WT mice; $^{\#\#\#}p<0.001$ vs. untreated SCA2 mice (one-way ANOVA with Tukey's post hoc analysis; n = 6 for each group). **F** A simple composite phenotype scoring system was used to evaluate WT and SCA2 mice at 4-week intervals after hMSC treatment. $^{*}p<0.05$ *vs*. untreated WT mice; $^{\#}p<0.05$ *vs*. untreated SCA2 mice (one-way ANOVA with Tukey's post-hoc analysis; Kruskal–Wallis test for average score; n = 6 for each group)

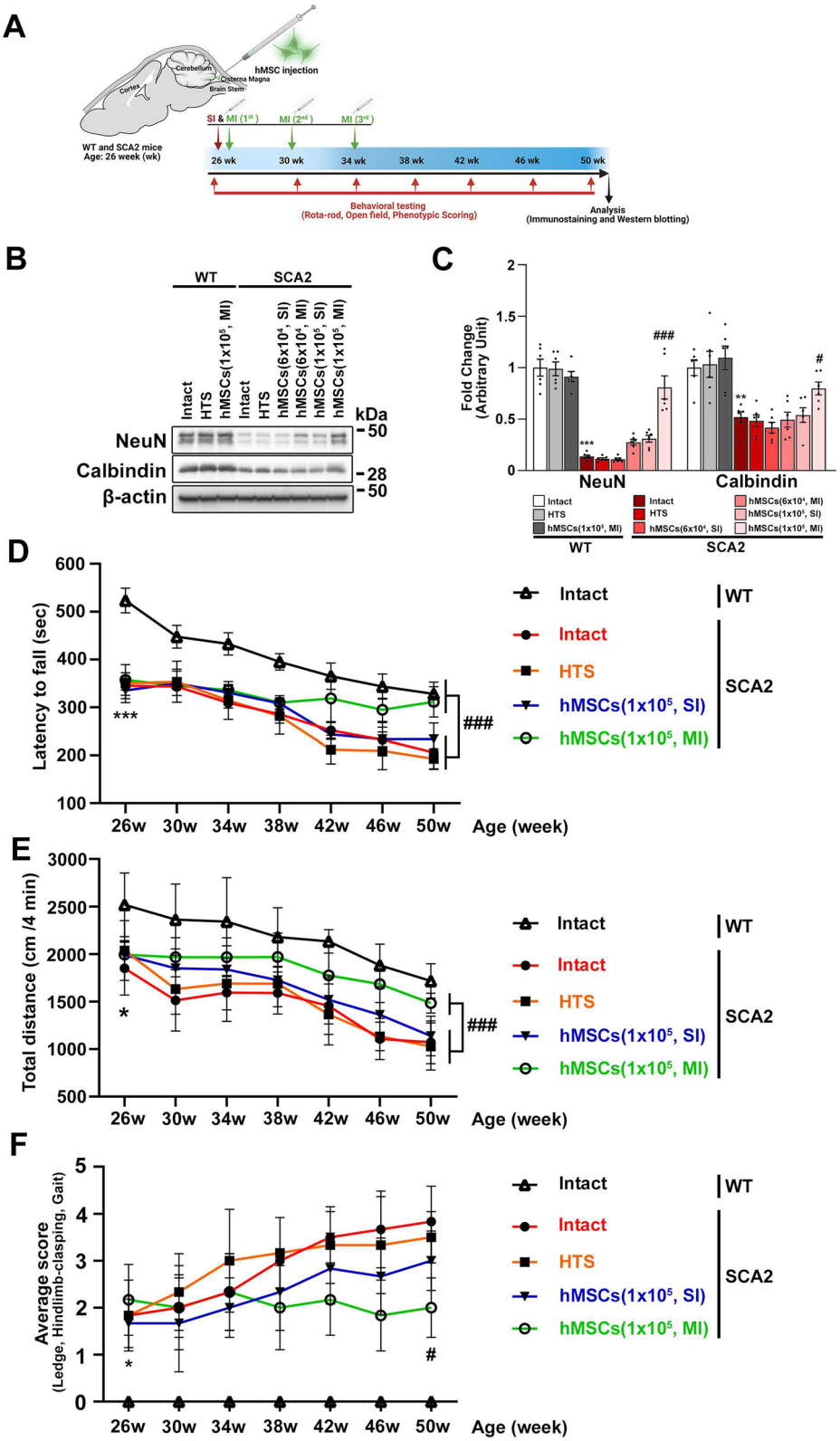

Fig. 1 (See legend on previous page.)

most severe symptoms. These individual test scores were then combined to obtain an overall composite phenotype score ranging from 0 to 9. Each test was performed three times at each time point to ensure the accuracy and consistency of the results.

Briefly, the ledge test [45, 46] was employed to estimate the degree of imbalance and lack of coordination by evaluating the mice's ability to walk along the cage ledge without losing balance. The following scoring system was used, where a score of 0 was given when the mouse walked normally along the ledge without losing its balance; a score of 1: when the mouse walked along the ledge with an asymmetrical posture; a score of 2: when the mouse loses footing while walking along the ledge; and a score of 3: when mouse does not effectively use its hind legs while walking. The hindlimb clasping test [45, 46] was used as a marker of disease progression, where scoring the mice was based on their hindlimb position when lifted by the tail. A score of 0 was given when the hindlimbs were consistently spread away from the abdomen. A score of 1, is when one hindlimb is retracted towards the abdomen for more than half of the test duration. A score of 2, when both hindlimbs are partially retracted towards the abdomen for more than half of the test duration. A score of 3, when both hindlimbs are completely retracted and touching the abdomen for over half of the test duration. The mice were assessed for their coordination and muscle function using a standardized gait test [45, 46], which involved placing them on a flat surface and observing their walking patterns. A scoring system was employed to evaluate their gait, with the following criteria: 0: Normal walking pattern; body weight supported evenly on all limbs; abdomen not touching the ground; 1: tremor or limping while walking; 2: severe tremor, severe limp, lowered pelvis, or duck walk observed during locomotion; 3: difficulty moving forward; dragging of the abdomen along the ground.

Immunofluorescence staining

The mice were anesthetized using a ketamine/xylazine mixture, followed by transcardial perfusion with 4% ice-cold paraformaldehyde (PFA) in 0.1 M PBS, as described previously [17]. The brains were then carefully extracted and post-fixed in 4% PFA overnight. Following this, the fixed brains were cryoprotected in a 30% sucrose solution for 24 h at 4 °C. Using an HM525 NX cryostat microtome (Thermo Fisher Scientific, Scoresby, VIC, Australia), the brains were sectioned into sagittal cerebellar sections of 30 μm thickness for immuno-fluorescence staining.

The free-floating cerebellar sections were washed in 0.1 M PBS and blocked with 0.5% BSA in PBS. They were then incubated overnight at 4 °C with specific primary antibodies, including mouse anti-calbindin-D-28 K (1:1000), mouse anti-NeuN (1:500), rabbit anti-BDNF (1:500), rabbit anti-GDNF (1:500), rabbit anti-FSTL1 (1:200), and rabbit anti-TGF-β1 (1:200). After rinsing, the sections were incubated with secondary fluorescently labeled IgG antibodies, including Texas Red-conjugated anti-mouse IgG (1:400), Texas Red-conjugated anti-rabbit IgG (1:400), FITC-conjugated anti-mouse IgG (1:400), and FITC-conjugated anti-rabbit IgG (1:400) for 1 h at room temperature. Finally, the sections were mounted using a Vectashield mounting medium and examined under a fluorescence microscope (Axio Imager; Carl Zeiss, Gottingen, Germany).

Co-localization analyses were performed, with certain modifications [47]. Briefly, to quantify the co-localizations, non-overlapping fields of view (200 μm × 200 μm) of the cerebellar area (Purkinje cell layer or Granule cell layer) were randomly selected as regions of interest. Moreover, a binary image of co-localized pixels from two separate channels (Calbindin/BDNF, Calbindin/GDNF, NeuN/BDNF, NeuN/GDNF, Calbindin/FSTL1, Calbindin/TGF-β1, NeuN/FSTL1, or NeuN/ TGF-β1) was generated on each field using Image J software and the co-localization plug-in. Co-localization was established for pixels whose intensities exceeded the threshold and for which the ratio of intensity was > 50%. Image J software was also used to automate channel thresholds. To compare the co-localization intensity between each group, the average pixel value of the WT intact fluorescence intensities was used as a reference and presented relative to the average values of the other groups.

Western blot analysis

Western blotting was performed using total cell lysates isolated from the cerebellum of mice, following previously established protocols [17, 48]. The obtained cerebellum tissues were homogenized in lysis buffer containing 58 mM Tris–HCl (pH 6.8); 10% glycerol; 2% SDS; protease inhibitor cocktail (1:100) and phosphatase inhibitor cocktail (1:100). After centrifugation of the lysate at 14,000 × g and 4 °C for 15 min, the supernatant was carefully transferred to a new tube, and the protein concentration was measured using a bicinchoninic acid assay kit (Bio-Rad Laboratories). Next, 50 μg of the protein sample was subjected to electrophoresis on a sodium dodecyl sulfate/polyacrylamide gel (Bio-Rad Laboratories) and subsequently transferred to polyvinylidene difluoride membranes (Millipore) using an electrophoretic transfer system (Bio-Rad Laboratories). The membranes were then incubated at 4 °C for 24 h with specific primary antibodies, including rabbit anti-calbindin (1:3000), mouse anti-neuronal nuclear protein (NeuN, 1:1000), rabbit anti-ionized calcium-binding adaptor molecule 1 (Iba1, 1:1000), rabbit anti-Ataxin-2 (1:2000)

rabbit anti-IL-1β (1:500), mouse anti-TNF-α (1:500), rabbit anti-inducible nitric oxide synthase (iNOS, 1:1000), rabbit anti-glial fibrillary acidic protein (GFAP, 1:2000), rabbit anti-BDNF (1:1000), rabbit anti-glial cell-derived neurotrophic factor (GDNF, 1:1000), rabbit anti-ciliary neurotrophic factor (CNTF, 1:1000), rabbit anti-FSTL1 (1:1000), rabbit anti-TGF-β1 (1:1000) and mouse anti-β-actin (1:1000). Following incubation, the membranes were washed and incubated with horseradish peroxidase-conjugated secondary antibodies, including anti-mouse IgG (1:4000) and anti-rabbit IgG (1:4000), at room temperature for 1 h. Protein bands were visualized using enhanced chemiluminescence western blot detection reagents (GE Healthcare Life Sciences), and the signal was analyzed using a LAS-500 image analyzer (GE Healthcare Life Sciences). The band density of the target protein was quantified using Multi-Gauge version 4.0 (Fuji Film), with normalization to the β-actin band intensity for each sample.

Statistical analysis

The data are presented as mean ± standard error of the mean. The experimental results were evaluated a priori using the Shapiro–Wilk normality test for Gaussian distribution. Differences between groups were evaluated using Student's t-test, one-way analysis of variance (ANOVA), or two-way ANOVA followed by Tukey's post hoc analysis. Non-parametric analyses, such as the Kruskal–Wallis and Friedman tests, were utilized, as appropriate. All statistical analyses were performed using IBM SPSS software (version 27.0.1.0; International Business Machines Corporation, Armonk, NY) and GraphPad Prism (version 8.30; GraphPad Software, San Diego, CA). The *p*-values of all figures are shown in Supplementary Table 2.

Results

Neuronal degeneration occurs in the cerebellum of 25-week-old SCA2 mice

Considering the limited identification of early-onset SCA2 [49–51] owing to the variability in symptom onset age, gradual symptom progression, and non-motor manifestations, we initially examined the time course of behavioral and biochemical changes in the cerebellum of SCA2 mice and compared it with that in WT mice (Supplementary Fig. 1). We next investigated the protein levels of NeuN (cerebellar granule cell marker) and calbindin (Purkinje cell marker) in the cerebellum tissues of SCA2 mice at 10, 25, and 50 weeks of age, comparing them with WT mice at the same time intervals (Supplementary Fig. 2 and Supplementary Table 1). Western blotting data showed that the protein levels of NeuN were significantly decreased in the cerebellum of 25- and 50-week-old SCA2 mice compared with those in WT mice (Supplementary Fig. 2; $^{**}p < 0.01$ and $^{***}p < 0.001$ vs. 10-week-old WT mice; n = 6 and Supplementary Table 1). The level of calbindin showed a similar time-dependent decline in SCA2 mice, being significantly decreased at 25 and 50 weeks (Supplementary Fig. 2; $^{**}p < 0.01$ and $^{***}p < 0.001$ vs. 10-week-old WT mice; n = 6 and Supplementary Table 1).

Multiple hMSC treatments mitigate Purkinje cell damage and impaired behaviors of SCA2 mice

To investigate the effects of hMSCs on cerebellar cell damage in SCA2 mice, we examined the protein levels of NeuN and calbindin in the cerebellum of hMSC-treated WT (only MI) and SCA2 mice (Fig. 1B,C). Western blotting showed a significant reduction in the protein levels of NeuN and calbindin in the cerebellum of untreated SCA2 mice at 50 weeks of age compared to untreated WT mice at the same age (Fig. 1B,C; $^{**}p < 0.01$ and $^{***}p < 0.001$ vs. untreated WT mice; n = 6). Although enhanced NeuN expression was observed at higher SI dosages, the protein levels of NeuN and calbindin were significantly preserved in the cerebellum at 50 weeks of age in SCA2 mice treated with MI of hMSCs (1×10^5 cells) compared with those in untreated, same-age SCA2 mice (Fig. 1B,C; $^{\#}p < 0.05$ and $^{\#\#\#}p < 0.001$ *vs.* untreated SCA2 mice; n = 6).

To explore the impact of hMSCs administration on motor coordination and gait abnormalities, we analyzed loss of locomotor function using the accelerating rotarod test. We observed that 26-week-old SCA2 mice exhibited a significant decline in retention time (344.83 ± 11.16 s) on the rotating rod compared to WT mice (523.33 ± 10.67 s) ($^{***}p < 0.001$ vs. untreated WT mice; n = 6; Fig. 1D). However, SCA2 mice treated with multiple hMSC injections (1×10^5 cells) showed preserved retention time (311.33 ± 12.98 s) on the rotating rod compared to untreated SCA2 mice at 50 weeks of age (205.83 ± 14.55 s) (Fig. 1D; $^{\#\#\#}p < 0.001$ vs. untreated SCA2 mice; n = 6). Single hMSC treatments did not prevent the observed behavioral impairment in SCA2 mice (Fig. 1D). Consistent with the rotarod results, the open-field test demonstrated that multiple hMSC treatments (1482.66 ± 42.89 cm) significantly reduced impairment of locomotor activity in SCA2 mice (1072.29 ± 92.39 cm) (Fig. 1E; $^{*}p < 0.05$ vs. untreated WT mice; $^{\#\#\#}p < 0.001$ vs. untreated SCA2 mice; n = 6). Furthermore, the phenotype scoring tests revealed that multiple hMSC treatments (2 ± 0.26) effectively mitigated motor impairment (determined by ledge and gait testing) and abnormal hindlimb clasping in SCA2 mice (3.83 ± 0.3) (Fig. 1F; $^{*}p < 0.05$ vs. untreated WT mice; $^{\#}p < 0.05$ vs. untreated SCA2 mice; n = 6).

hMSC treatment in SCA2 mice leads to elevated protein levels of neurotrophic factors and inhibits Purkinje cell degeneration

To explore the changes in protein expression of neurotrophic factors such as BDNF, GDNF, and CNTF, we first performed western blot analysis on cerebellar tissues from WT and SCA2 mice at 10 weeks, 25 weeks, and 50 weeks of age (Supplementary Fig. 3A,B). Our results revealed a significant decrease in the levels of BDNF, GDNF, and CNTF in the cerebellum of 25- and 50-week-old SCA2 mice compared to WT mice (Supplementary Fig. 3A, B; $^{**}p<0.01$ and $^{***}p<0.001$ vs. 10-week-old WT mice and Supplementary Table 1; n = 6). Next, to assess the potential association between hMSC treatment-induced behavioral improvement and neurotrophic factors, we examined the protein levels of BDNF, GDNF, and CNTF in the cerebellum of SCA2 mice after hMSC administration (Fig. 2A,B). Western blot results revealed a significant decrease in the protein levels of BDNF, GDNF, and CNTF in the cerebellum of SCA2 mice compared to untreated WT mice (Fig. 2A,B; $^{***}p<0.001$ vs. untreated WT mice; n = 6). However, the protein levels of these neurotrophic factors were preserved in the cerebellum of SCA2 mice treated with multiple hMSC injections (1×10^5 cells) when compared to untreated SCA2 mice at 50 weeks of age (Fig. 2A,B; $^{###}p<0.001$ vs. untreated SCA2 mice n = 6).

The effect of multiple hMSC injections on BDNF and GDNF expression was also evaluated via double immunofluorescence staining (Fig. 2C–F). Results revealed that hMSC treatment preserved trophic factors with calbindin-positive cells in the Purkinje cell layer (PCL). The results obtained using double immunofluorescence staining (Fig. 2C,E) indicate significant colocalization of calbindin with BDNF and GDNF in the PCL. The fluorescence intensity for the quantitative co-localization of calbindin with BDNF and GDNF revealed that hMSC treatment preserved BDNF and GDNF with calbindin-positive cells in the PCL (Fig. 2D,F; $^{***}p<0.001$ *vs.* untreated WT mice at 50 weeks of age; $^{###}p<0.001$ *vs.* untreated SCA2 mice at 50 weeks of age; n = 6). However, no significant co-localization of NeuN with BDNF and GDNF was observed in the granule cell layer (GCL) (Supplementary Fig. 3C–F).

hMSC treatment in SCA2 mice exerts anti-inflammatory effects in the cerebellum

Since neuroinflammation is a major feature of SCA2, we next asked whether hMSC administration can inhibit prolonged neuroinflammation, investigating the expression of glial cell markers Iba1 and GFAP in the cerebellum of SCA2 mice. We first investigated the potential changes in protein expression of neurotoxic molecules such as TNF-α, IL-1β, and iNOS, mediated by the activation of glial cells in an age-dependent manner. We conducted western blot analysis on cerebellar tissues obtained from WT and SCA2 mice at 10, 25, and 50 weeks of age (Supplementary Fig. 4 and Supplementary Table 1). The western blot result revealed a significant increase in the protein levels of Iba1, a microglia marker, and GFAP, an astrocyte marker, in the cerebellum of 50-week-old SCA2 mice compared to those in WT mice (Supplementary Fig. 4A, B; $^{**}p<0.01$ and $^{***}p<0.001$ vs. 10-week-old WT mice; n = 6). The protein levels of TNF-α, IL-1 β, and iNOS were also increased in the cerebellum of 25- and 50-week-old SCA2 mice (Supplementary Fig. 4C,D; $^{***}p<0.001$ vs. 10-week-old WT mice; n = 6). However, the protein levels of Iba1 and GFAP were decreased in the cerebellum of SCA2 mice treated with multiple hMSC injections (1×10^5 cells) compared to untreated SCA2 mice at 50 weeks of age (Fig. 3A,B; $^{###}p<0.001$ vs. untreated SCA2 mice; n = 6). Consistent with the decrease in glial cell presence, the protein levels of TNF-α, IL-1 β, and iNOS were also reduced in the cerebellum of SCA2 mice treated with multiple hMSC injections (1×10^5 cells) compared to untreated SCA2 mice at 50 weeks of age (Fig. 3C,D; $^{***}p<0.001$ vs. untreated WT

(See figure on next page.)

Fig. 2 Treatment with hMSCs upregulates the protein levels of neurotrophic factors in the cerebellum of SCA2 mice. **A**, **B** Western blot analysis of brain-derived neurotrophic factor (BDNF), glial cell-derived neurotrophic factor (GDNF), and ciliary neurotrophic factor (CNTF) in the cerebellum after 24 weeks of hMSC administration (50-week-old mice). $^{***}p<0.001$ *vs.* untreated WT mice; $^{###}p<0.001$ *vs.* untreated SCA2 mice (two-way ANOVA with Tukey's post-hoc analysis; n = 6 for each group). Full-length blots are presented in Supplementary Fig. 5 and Fig. 2A. **C** Double immunofluorescence staining was performed for calbindin and BDNF in the cerebellum of 50-week-old WT, SCA2, and SCA2 + hMSCs (MI, 1×10^5 cells)-treated mice. The scale bar represents 20 μm. A dashed line is used to differentiate between the granule cell layer and the Purkinje cell layer. **D** The fluorescence intensity for the quantitative co-localization of calbindin with BDNF and GDNF was measured. $^{***}p<0.001$ *vs.* untreated WT mice; $^{###}p<0.001$ *vs.* untreated SCA2 mice (one-way ANOVA with Tukey's post-hoc analysis). **E** Double immunofluorescence staining was performed for calbindin and GDNF in the cerebellum of 50-week-old WT, SCA2, and SCA2 + hMSCs (MI, 1×10^5 cells)-treated mice. The scale bar represents 20 μm. A dashed line is used to differentiate between the granule cell layer and the Purkinje cell layer. **F** The fluorescence intensity for the quantitative co-localization of calbindin with GDNF was measured. $^{***}p<0.001$ *vs.* untreated WT mice; $^{###}p<0.001$ *vs.* untreated SCA2 mice (one-way ANOVA with Tukey's post-hoc analysis)

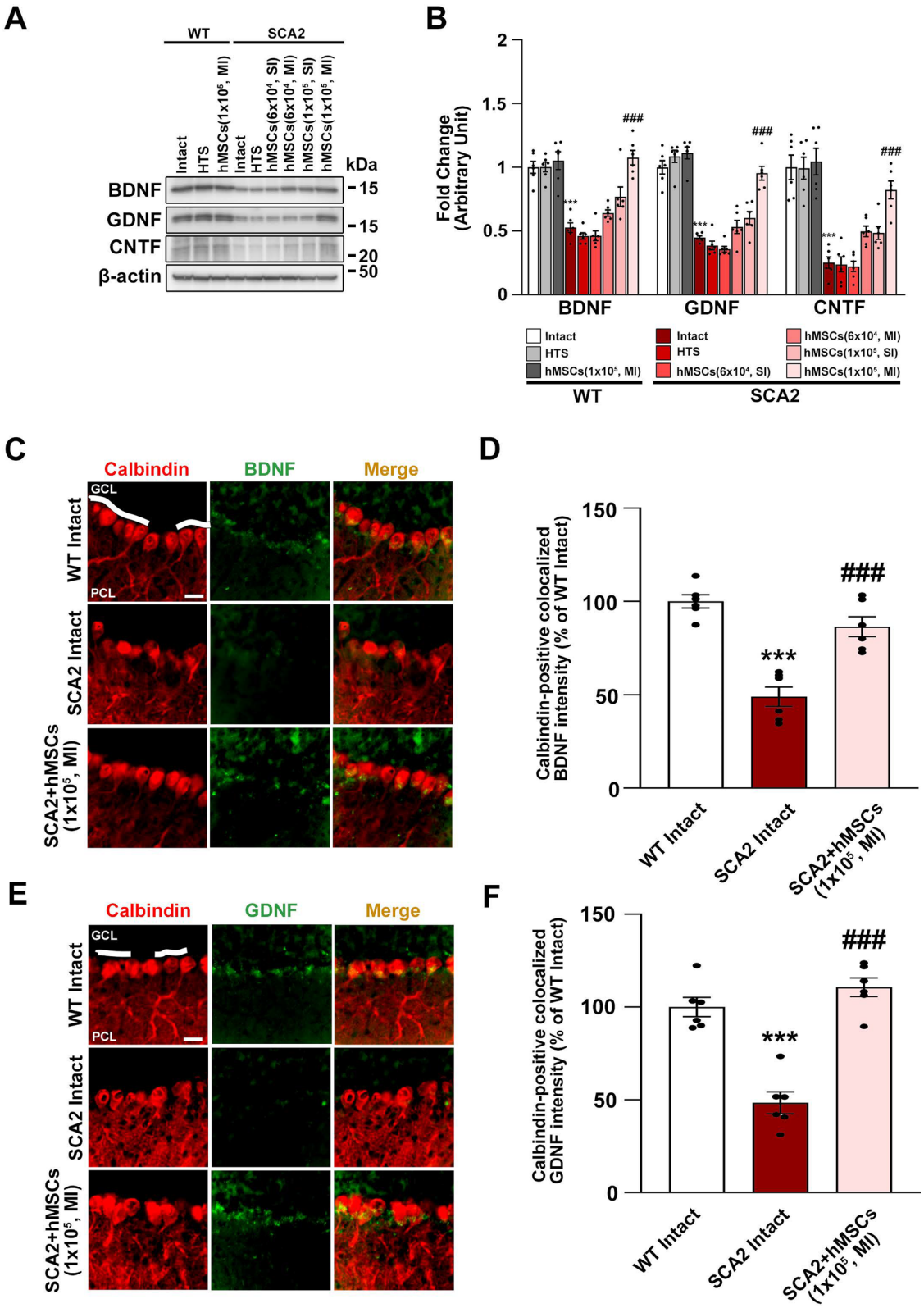

Fig. 2 (See legend on previous page.)

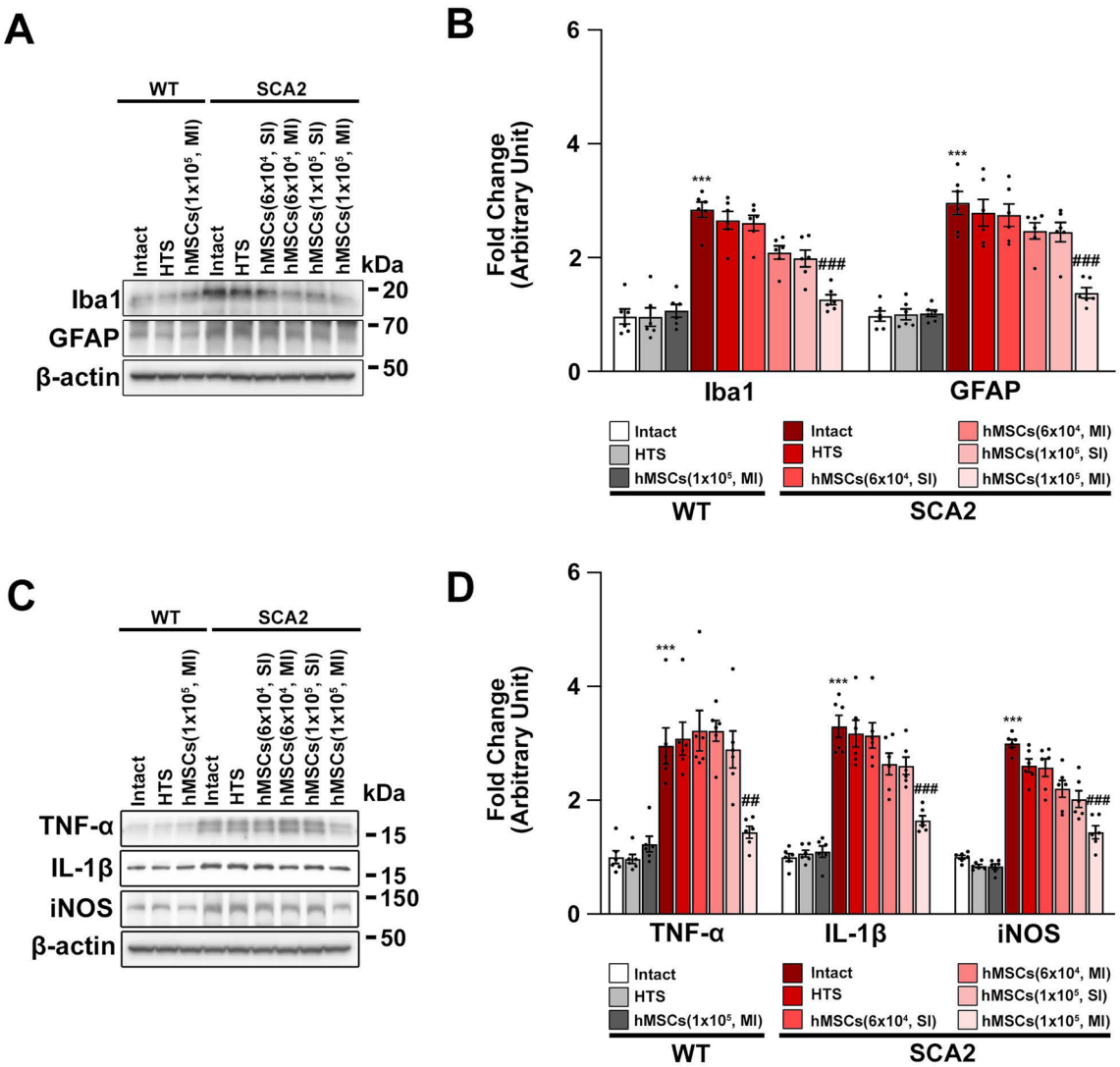

Fig. 3 Treatment with hMSCs downregulates the protein levels of glial-mediated neurotoxic cytokines in the cerebellum of SCA2 mice. **A**, **B** Western blot analysis of ionized calcium-binding adaptor molecule 1 (Iba1) and glial fibrillary acidic protein (GFAP) in the cerebellum after 24 weeks of hMSC administration (50-week-old mice). $^{***}p<0.001$ vs. untreated WT mice; $^{###}p<0.001$ vs. untreated SCA2 mice (two-way ANOVA with Tukey's post hoc analysis; n = 6 for each group). Full-length blots are presented in supplymentary Fig. 5: Fig. 3A. **C**, **D** Western blot analysis of tumor necrosis factor-alpha (TNF-α), interleukin-1 beta (IL-1β), and inducible nitric oxide synthase (iNOS) in the cerebellum after 24 weeks of hMSC administration (50-week-old mice). $^{***}p<0.001$ vs. untreated WT mice; $^{##}p<0.01$ and $^{###}p<0.001$ vs. untreated SCA2 mice (two-way ANOVA with Tukey's post hoc analysis; n = 6 for each group). Full-length blots are presented in supplymentary Fig. 5: Fig. 3C

mice; $^{##}p<0.01$ and $^{###}p<0.001$ vs. untreated SCA2 mice; n = 6).

Preservation of FSTL1 and TGF-β1 in the cerebellum by hMSC treatment in SCA2 mice

While studying the signaling cascades mediated by hMSC administration, we assessed the cerebellar protein expression of FSTL1 and binding partner, TGF-β1, which are associated with neuroinflammation and neurotrophic factors. Decreases in FSTL1 and TGF-β1 levels were first observed at 25 weeks and were significantly reduced with progression of the disease (Fig. 4A,B; $^{**}p<0.001$ and $^{***}p<0.001$ vs. 10-week-old WT mice and Supplementary Table 1; n = 6). Decreases in FSTL1 and TGF-β1 levels were also observed in calbindin-positive and NeuN-positive cells (Fig. 4C–F; $^{***}p<0.001$ *vs.* untreated WT mice at 50 weeks of age; n = 6). Multiple hMSC (1×10^5 cells) treatments, however, preserved the protein levels of FSTL1 and TGF-β1 in the cerebellum of SCA2 mice (Fig. 4G,H; $^{***}p<0.001$ vs. untreated

WT mice; $^{###}p < 0.001$ vs. untreated SCA2 mice; n = 6). Comprehensively, these results suggest that hMSC treatments upregulate the protein expression of FSTL1, which is associated with reducing inflammation and regulating neurotrophic factors, leading to improvements in both the behavioral and physiological aspects of the SCA2 phenotype (Fig. 4I).

Discussion

In the context of SCA2, a complex interplay exists between neurotrophic factors and neuroinflammation. While BDNF, GDNF, and other factors like CNTF can modulate neuroinflammation, chronic inflammatory processes can further deplete their levels, potentially creating a detrimental feedback loop that contributes to neurodegeneration and SCA2 progression. Recent studies have indicated the involvement of neuroinflammatory responses, characterized by the production of inflammatory cytokines from activated microglia and astrocytes, in SCA2 disease progression in both patients and animal models [31, 52]. Interestingly, this increase in microglial number and inflammatory cytokine levels occurs early in the disease process, suggesting a potential mechanism of neurodegeneration driven by microglia-mediated inflammation [17, 52, 53]. We recently reported that hMSC treatment significantly inhibited the symptoms of ataxia in LPS- [17] and Ara-C- [18] induced inflammatory CA and showed that FSTL1 and TGF-β1 was downregulated in the CA-MSC secretome with suppressive effects on microglial activation [31]. Herein, we aimed to explore the potential therapeutic benefits of hMSC injection in a preclinical SCA2 mouse model and investigate the potential role of FSTL1 in mediating these effects. Intriguingly, a reduction in FSTL1 levels was paradoxically associated with increased neuroinflammation, decreased levels of neurotrophic survival factors, and subsequent motor impairment. Conversely, the increase in FSTL1 levels after hMSC administration was accompanied by alleviation of inflammatory responses and cell death, further supporting the notion that FSTL1 signaling may play a significant role in SCA2 pathology and potentially serve as a target in the development of new therapeutics for SCA2 treatment.

Identifying early SCA2 is challenging due to the variability in age of symptom onset, gradual symptom progression, and non-motor manifestations [49–51]. However, studying 25-week-old mice generally corresponds to a stage in disease progression that mirrors the onset of symptoms, such as the presence of toxic polyQ aggregates, degeneration of Purkinje cells, and development of motor abnormalities, observed in human patients with SCA2 [37–42]. To address the challenges associated with accurately identifying SCA2 onset, we initially confirmed SCA2 symptoms using age-dependent behavioral patterns as well as gene and protein analysis [34, 35]. By 25 weeks of age, the SCA2 mice in our study began to exhibit motor symptoms, such as impaired coordination, balance problems, gait abnormalities, and the progressive degeneration of cerebellar neurons; these symptoms significantly increased with disease progression [37] (Fig. 1F and Supplementary Fig. 2). Additionally, we observed a loss of neurotrophic factors (Supplementary Fig. 3A, B) [1, 18, 51] accompanied by increased inflammatory responses over the course of disease progression by 50 weeks of age [1, 17, 18, 54] (Supplementary Fig. 4). Hence, hMSCs were injected in 26-week-old mice, and protein levels of neurotrophic factors, inflammatory molecules, and cytokines were monitored in 50-week-old mice after 24 weeks of hMSC administration (Fig. 2 and 3).

hMSCs have been reported to enhance motor function, including coordination, balance, and.

motor skills, and exhibit overall neuroprotective effects in not only preclinical animal models [15, 18] but also

(See figure on next page.)

Fig. 4 hMSC treatment preserves the protein levels of follistatin-like 1 (FSTL1) and transforming growth factor beta 1 (TGF-β1) in the cerebellum of SCA2 mice. **A**, **B** Western blot analysis of FSTL1 and TGF-β1 in cerebellum tissues obtained from 10-, 25-, and 50-week-old WT and SCA2 mice. $^{**}p < 0.001$ and $^{***}p < 0.001$ vs. 10-week-old WT mice (two-way ANOVA with Tukey's post hoc analysis; n = 6 for each group). Full-length blots are presented in supplementary Fig. 5; Fig. 4A. **C** Double immunofluorescence staining was performed for calbindin and FSTL1 as well as calbindin and TGF-β1 in the cerebellum of 50-week-old WT and SCA2 mice. The scale bar represents 20 μm. The dashed line differentiates between the granule and Purkinje cell layers. **D** The fluorescence intensity for the quantitative co-localization of calbindin with FSTL1 and TGF-β1 was measured. $^{***}p < 0.001$ *vs*. untreated WT mice (t-test with Tukey's post-hoc analysis). **E** Double immunofluorescence staining was performed for NeuN and FSTL1 as well as NeuN and TGF-β1 in the cerebellum of 50-week-old WT and SCA2 mice. The scale bar represents 20 μm. The dashed line differentiates between the granule and Purkinje cell layers. **F** The fluorescence intensity for the quantitative co-localization of NeuN with FSTL1 and TGF-β1 was measured. $^{***}p < 0.001$ *vs*. untreated WT mice (t-test with Tukey's post-hoc analysis). **G**, **H** Western blot analysis of FSTL1 and TGF-β1 in the cerebellum after 24 weeks of hMSC administration (50-week-old mice). $^{***}p < 0.001$ vs. untreated WT mice; $^{###}p < 0.001$ vs. untreated SCA2 mice (two-way ANOVA with Tukey's post hoc analysis; n = 6 for each group). Full-length blots are presented in supplymentary Fig. 5: Fig. 4G. **I** Schematic representation of the effects of hMSCs in the SCA2 model. hMSC administration upregulates the expression of FSTL1, which in turn reduces inflammation and is accompanied by behavioral and physiological improvements in the SCA2 phenotype. The figure was created using BioRender.com (Agreement number: BG25IEMZTA)

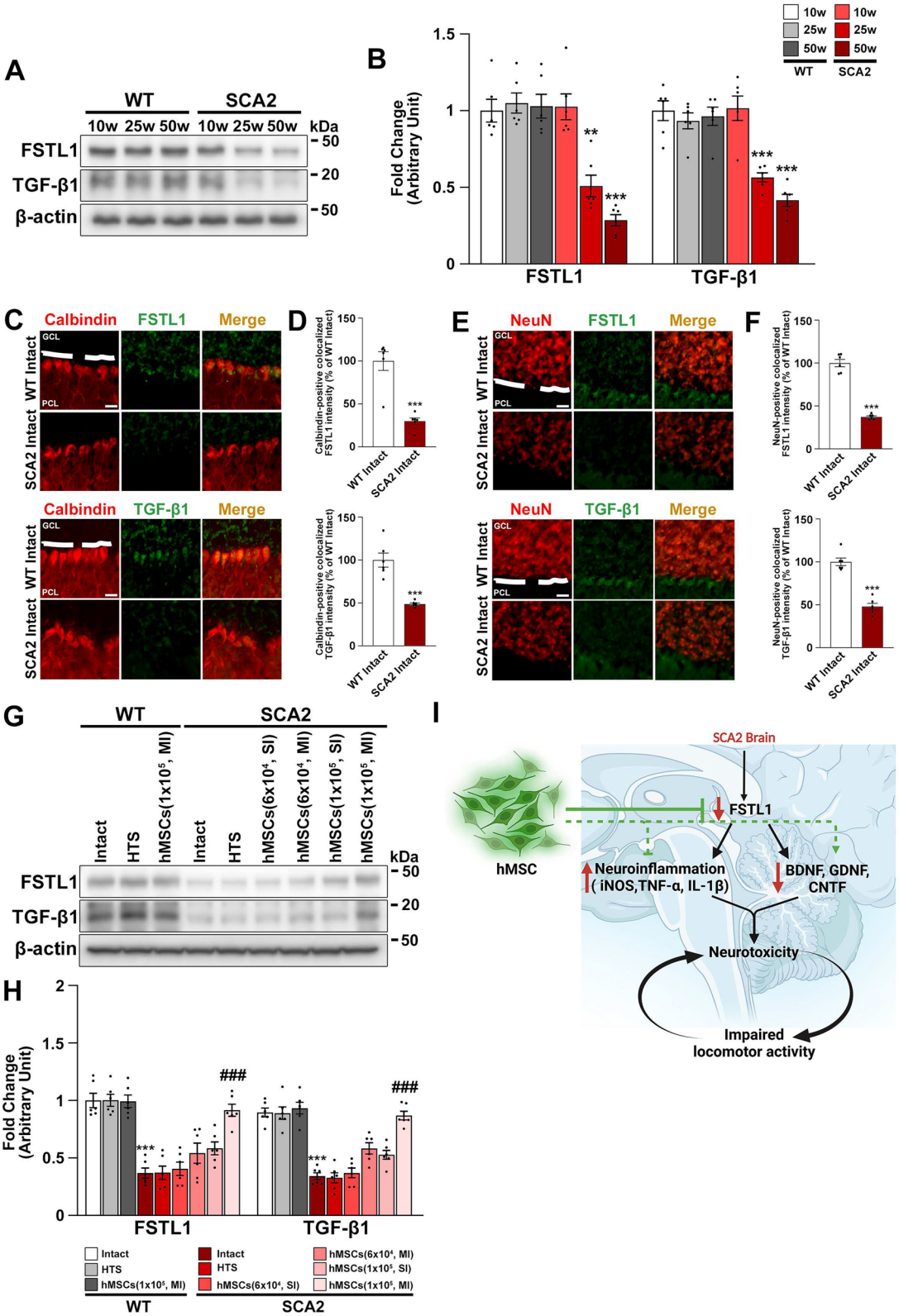

Fig. 4 (See legend on previous page.)

human clinical trials [16]. Moreover, the administration of hMSCs has been shown to exert various effects on neighboring cells through the release of cytokines, chemokines, and growth factors [55–57]. hMSCs also show anti-inflammatory and immune-modulating effects via the secretion of growth factors and other immune mediators [58] which can further activate endogenous mechanisms for tissue repair and regeneration while promoting cell survival. Purkinje cell dysfunction and death are key contributors to motor impairments observed in SCA2. Calbindin, primarily derived from Purkinje cells, is often used as a marker to assess the presence and health of these cells [59]. Elevated calbindin levels may suggest a healthier population of Purkinje cells, while a decline may correlate with the severity of Purkinje cell-related ataxia [60]. Interestingly, neurotrophic factors like BDNF, GDNF, and CNTF can influence calbindin expression [61–63]. These factors are known to support existing neurons and promote the growth and differentiation of new ones by activating common intracellular signaling pathways [64, 65]. Earlier reports suggest that mice with targeted gene deletion of BDNF exhibit a wide-based gait along with increased death of granule cells, stunted growth of Purkinje cell dendrites, impaired formation of horizontal layers, and defects in the rostral–caudal foliation pattern [66]. These effects are accompanied by reduced activation of its receptor, tropomyosin receptor kinase B (TrkB), in both granule and Purkinje cells, indicating that BDNF directly affects these cell types [66]. Moreover, BDNF increases the spine density of the surviving Purkinje cells in vitro [67]. BDNF plays a role in regulating the mechanisms underlying short-term synaptic plasticity and the steady-state relationship between different vesicle pools within the pre-synaptic terminal in the cerebellum [68].

Studies conducted with human samples from patients with multiple system atrophy have indicated that GDNF is primarily synthesized and localized within the Purkinje cells of the human cerebellum [69], where it reportedly increases the proportion of Purkinje cells displaying relatively mature morphologies, characterized by dendritic thickening and the development of spines and filopodial extensions [70]. Similarly, CNTF plays a crucial role in the survival, differentiation, and potential repair of Purkinje cells, contributing to proper cerebellar function, thus aiding in motor coordination, balance, and motor learning [71]. Notably, hMSCs can directly produce BDNF, GDNF, and CNTF, which can positively influence calbindin levels in the ataxic brain [18, 69, 72–74]. Consistent with previous studies [15, 16], our findings revealed that hMSC administration improves motor function and leads to an elevation in BDNF, GDNF, and CNTF levels, thus protecting cerebellar neurons from cell death. Further, our study demonstrates that calbindin-positive cells in the PCL express BDNF and GDNF (Fig. 2C–F). Despite observing the strong immunoreactivity of BDNF in the GCL, we found no significant colocalization between BDNF and NeuN-positive cells in the GCL (Supplementary Fig. 3C–F). Furthermore, the absence of colocalization between NeuN and GDNF in the GCL supports the notion that trophic factors such as GDNF and BDNF are primarily localized and expressed in Purkinje cells [69]. Reportedly, CNTF also predominantly are expressed by Purkinje cells [75]. These findings underscore the potential of hMSCs as a valuable tool supporting trophic factors in developing novel therapeutic strategies for SCA2 showing the loss of trophic factors in PCL. Besides, it raises important questions about the mechanisms by which hMSC-mediated secretion of growth survival factors can aid in Purkinje cell health thus impacting locomotion and motor coordination.

Currently, the precise mechanism underlying the interaction between hMSCs and host tissue, leading to the stimulation of neurotrophin expression, remains unclear. Previous studies have demonstrated that hMSC transplantation induces cell proliferation in neurogenic zones and facilitates the migration of neural progenitors to damaged areas, resulting in the production of neurotrophins and subsequent damage recovery [76–78]. However, the specific signaling pathways involved in this process require further investigation. Earlier reports have suggested that FSTL1 may interact with, and be regulated by, neurotrophic factors, such as BDNF, GDNF, and CNTF [79–82]. BDNF can upregulate FSTL1 expression in cardiac fibroblasts [82]. Additionally, FSTL1 has been reported to enhance the pro-survival effects of BDNF on neurons [24] and act downstream of BDNF-signaling pathways to promote cell survival and inhibit apoptosis in certain neuronal cell and mouse models [24, 26, 28, 83]. Another report suggested that the neuroprotective effects of FSTL1 are comparable to those of GDNF in reducing dopaminergic cell loss [84]. Moreover, FSTL1 expression was increased after CNTF treatment, suggesting the potential involvement of FSTL1 in CNTF-mediated neuroprotection [85, 86]. Treatment with both GDNF and CNTF increases FSTL1 expression in astrocytes, suggesting their potential interplay in glial cell function [79, 80]. We found that hMSC treatment promotes FSTL1 activation, which in turn is associated with a reduction of proinflammatory cytokines in the mouse brain (Fig. 3C, 3D, 4G, and 4H). Moreover, we identified reduced expression levels of FSTL1 and TGF-β1 in SCA2 mice (Fig. 4C–H), suggesting that FSTL1 loss may serve an essential role in behavioral impairment and inflammatory responses. However, at present, the underlying mechanisms connecting FSTL1 to motor impairment

and inflammation are unclear, and further research is warranted.

Recent studies have provided evidence of the crucial role of FSTL1 in various neurological conditions [87, 88]. Genetic knockdown of *Fstl1* in the hippocampus has been associated with impairments in learning and memory, as well as abnormal neural oscillations and synaptic plasticity [89]. Another previous report suggested that FSTL1 may modulate the activation of glial cells by reducing the expression of proinflammatory cytokines such as TNF-α and IL-1β via blockage of the MAPK/p-ERK1/2 pathway in astrocytes and NF-κB pathway in microglia, thus playing an inhibitory role in early neuroinflammation [22, 90, 91]. Furthermore, FSTL1 has been shown to shift microglial phenotypes toward an anti-inflammatory, M2-like state, aiding in tissue repair through the production of anti-inflammatory cytokines [17, 31]. FSTL1 has also been shown to enhance microglial phagocytosis, the process by which microglia engulf and clear cellular debris, pathogens, and toxic substances [92]. Previous studies have demonstrated its ability to enhance neuronal survival, promote the growth of neurites, and provide cellular protection against oxidative stress [93]. Altogether, these findings highlight the neuroprotective properties of FSTL1, underscoring its significance in the suppression of microglia-mediated inflammation and the maintenance of central nervous system homeostasis.

As we demonstrate here, one likely mechanism for SCA2 pathology is the release of cytokines, such as TNF-α and IL-1β, under the control of FSTL1 signaling. We establish that hMSC treatment promotes the activation of TGF-β/FSTL1, which affects immune cells by activating downstream signaling molecules (Fig. 4G,H). FSTL1 reportedly works synergistically with TGF-β1 and is responsible for its activation and enhanced expression [94]. Working together, FSTL1 and TGF-β1 are involved in the regulation of growth, differentiation, and survival of various cell types in multiple regions of the brain [94]. Notably, TGF-βs have been shown to inhibit the activity of microglial cells, thereby exerting an anti-inflammatory effect. Since microglial cells are a significant source of TGF-β1 in the central nervous system [95], TGF-β1 may exert self-inhibitory control [96]. Furthermore, elevated levels of TGF-β1 downregulate the expression of certain inflammatory proteins, suggesting that the neuroprotective effect of TGF-β1 may be attributable to the inhibition of chemokines during brain injury [97].

The results of our study align with those of others and our previous findings, indicating that a single transplantation of hMSCs merely exerts temporary effects [16, 18]. However, multiple administrations of hMSCs led to long-lasting improvements in motor behavior and alleviation of neuropathology in the Ara-C mouse model of CA [18]. Our study expands on this previous work by demonstrating that multiple injections of hMSCs result in increased FSTL1 levels and reduced inflammation (Fig. 3 and 4). Considering our previous studies, the present data indicate that repeated hMSC intrathecal administration potentially alleviates the SCA2 phenotype by preserving Purkinje cells and other paracrine effects (Figs. 1 and 2) [18]. These findings underscore the critical role of hMSC administration dosage and timing. Interestingly, the mode of hMSC administration significantly influences its efficacy, tolerability, and overall outcome. For instance, intravenous hMSC transplantation markedly delayed the onset of motor function decline in a preclinical SCA2 mouse model, while intracranial administration failed to demonstrate a comparable neuroprotective effect [15]. Similar findings were obtained in a phase I/IIa clinical study [16]. Additionally, intrathecal hMSC delivery via the cisterna magna resulted in the widespread distribution of hMSCs throughout the cerebrospinal fluid and cerebellum, contributing to improved ataxia symptoms [17]. Given the short lifespan of hMSCs and the progressive nature of SCA2, therapeutic strategies likely yield optimal results when implemented during the presymptomatic or prodromal stages. Understanding this timing element may also shed light on why some patients experience regression to pre-transplantation states a few months post-treatment [16]. Our results, and those of others, suggest that hMSC therapies should be redesigned to get sustained beneficial results in clinical practices [16, 98].

Conclusions

As our study was limited in its ability to (1) determine whether this pathway operates the same way in the presence of specific inhibitors and (2) examine the significance of FSTL1, further research into how gain-of-function and loss-of-function of FSTL1 and/or TGF-β1 impacts MSC-associated outcomes in preclinical models is required. Furthermore, whether FSTL1 requires any other binding for its activity remains unknown. Moreover, understanding the mechanisms underlying the involvement of FSTL1 in mitigating neuroinflammation, enhancing neurotrophic factors, and contributing to the deceleration of SCA2 progression warrants further investigation. Therefore, we cannot rule out the possibility that another mechanism may also be involved in the hMSC-induced preservation of motor activity decline. However, the present study reveals that hMSC treatment significantly ameliorated SCA2 symptoms in a mouse model, and the beneficial effects were related to the activation of the FSTL1-mediated preservation of Purkinje cells, which is associated with decreasing levels of proinflammatory molecules and

the activation of neurotrophic factors (Fig. 4I). Thus, our findings hold considerable clinical implications, suggesting that the administration of hMSCs could be a potential therapeutic strategy for SCA2 patients.

Abbreviations

SCA2	Spinocerebellar ataxia type 2
CA	Cerebellar ataxia
hMSCs	Human bone marrow-derived mesenchymal stem cells
LPS	Lipopolysaccharide
Ara-C	Cytosine β-D-arabinofuranoside hydrochloride
TSG-6	Tumor necrosis factor-stimulated gene-6
FSTL1	Follistatin-like protein 1
TGF-β1	Transforming growth factor-beta 1
BDNF	Bone-derived neurotrophic factor
TrkB	Tropomyosin receptor kinase B
GDNF	Glial cell-derived neurotrophic factor
CNTF	Ciliary neurotrophic factor
TNF-α	Tumor necrosis factor-alpha
IL-1β	Interleukin-1 beta
IL-6	Interleukin-6
Iba1	Ionized calcium-binding adaptor molecule 1
NeuN	Neuronal nuclear
GFAP	Glial fibrillary acidic protein
WT	Wild-type
HTS	HypoThermosol
SI	Single injection
MI	Multiple injection
ANOVA	Analysis of variance
GCL	Granule cell layer

Supplementary Information

The online version contains supplementary material available at https://doi.org/10.1186/s13287-024-04020-8.

Supplementary file 1.

Author contributions

SK: Conceptualization, methodology, investigation, formal analysis, visualization. CS: Investigation, formal analysis, visualization, writing—original draft. JH: Conceptualization, methodology. J-HK: Resources. YN: Formal analysis. MSK: Resources. TYL: Resources. K-SK: Resources. KS: Resources. H-WL: Resources. SRK: Conceptualization, methodology, investigation, formal analysis, visualization, project administration, supervision, writing—original draft, writing—review and editing.

Funding

This research was supported by the grants of Korea Health Industry Development Institute (HI16C2210 and HI21C1795) funded by the Korean government.

Availability of data and materials

All data generated or analysed during this study are included in this published article [and its supplementary information files].

Declarations

Ethics approval and consent to participate

The study was approved and conducted in accordance with the approved protocols of the Institutional Review Board of Chilgok Kyungpook National University Hospital [IRB: 2019–02-008-002 (Approved project title: Evaluation of the efficacy and safety of allogeneic bone marrow-derived mesenchymal stem cells in cerebellar ataxia), with approval obtained on May 15, 2019]. Written informed consent was obtained from all human subjects involved in the study.

Consent for publication

All authors approved the publication for this manuscript.

Competing interests

The authors declare no competing financial and non-financial interests.

Received: 4 March 2024 Accepted: 29 October 2024
Published online: 09 November 2024

References

1. Schols L, Bauer P, Schmidt T, Schulte T, Riess O. Autosomal dominant cerebellar ataxias: clinical features, genetics, and pathogenesis. Lancet Neurol. 2004;3:291–304.
2. Auburger GW. Spinocerebellar ataxia type 2. Handb Clin Neurol. 2012;103:423–36.
3. Seidel K, Siswanto S, Brunt ER, den Dunnen W, Korf HW, Rub U. Brain pathology of spinocerebellar ataxias. Acta Neuropathol. 2012;124:1–21.
4. Sinha KK, Worth PF, Jha DK, Sinha S, Stinton VJ, Davis MB, Wood NW, Sweeney MG, Bhatia KP. Autosomal dominant cerebellar ataxia: SCA2 is the most frequent mutation in eastern India. J Neurol Neurosurg Psychiatry. 2004;75:448–52.
5. Lo RY, Figueroa KP, Pulst SM, Lin CY, Perlman S, Wilmot G, Gomez CM, Schmahmann J, Paulson H, Shakkottai VG, Ying SH, Zesiewicz T, Bushara K, Geschwind M, Xia G, Subramony SH, Ashizawa T, Kuo SH. Vascular risk factors and clinical progression in spinocerebellar ataxias. Tremor Other Hyperkinet Mov. 2015;5:287.
6. Antenora A, Rinaldi C, Roca A, Pane C, Lieto M, Sacca F, Peluso S, De Michele G, Filla A. The multiple faces of spinocerebellar ataxia type 2. Ann Clin Transl Neurol. 2017;4:687–95.
7. Lastres-Becker I, Rub U, Auburger G. Spinocerebellar ataxia 2 (SCA2). Cerebellum. 2008;7:115–24.
8. Estrada R, Galarraga J, Orozco G, Nodarse A, Auburger G. Spinocerebellar ataxia 2 (SCA2): morphometric analyses in 11 autopsies. Acta Neuropathol. 1999;97:306–10.
9. Si YL, Zhao YL, Hao HJ, Fu XB, Han WD. MSCs: Biological characteristics, clinical applications and their outstanding concerns. Ageing Res Rev. 2011;10:93–103.
10. Staff NP, Jones DT, Singer W. Mesenchymal stromal cell therapies for neurodegenerative diseases. Mayo Clin Proc. 2019;94:892–905.
11. Zakrzewski W, Dobrzynski M, Szymonowicz M, Rybak Z. Stem cells: past, present, and future. Stem Cell Res Ther. 2019;10:68.
12. El-Kadiry AE, Rafei M, Shammaa R. Cell therapy: types, regulation, and clinical benefits. Front Med. 2021;8:756029.
13. In't Anker PS, Scherjon SA, Kleijburg-van der Keur C, de Groot-Swings GM, Claas FH, Fibbe WE, Kanhai HH. Isolation of mesenchymal stem cells of fetal or maternal origin from human placenta. Stem Cells. 2004;22:1338–45.
14. Joshi M, Patil PB, He Z, Holgersson J, Olausson M, Sumitran-Holgersson S. Fetal liver-derived mesenchymal stromal cells augment engraftment of transplanted hepatocytes. Cytotherapy. 2012;14(6):657–69.
15. Chang YK, Chen MH, Chiang YH, Chen YF, Ma WH, Tseng CY, Soong BW, Ho JH, Lee OK. Mesenchymal stem cell transplantation ameliorates motor function deterioration of spinocerebellar ataxia by rescuing cerebellar Purkinje cells. J Biomed Sci. 2011;18:54.
16. Tsai YA, Liu RS, Lirng JF, Yang BH, Chang CH, Wang YC, Wu YS, Ho JH, Lee OK, Soong BW. Treatment of spinocerebellar ataxia with mesenchymal stem cells: a phase I/IIA clinical study. Cell Transplant. 2017;26:503–12.
17. Nam Y, Yoon D, Hong J, Kim MS, Lee TY, Kim KS, Lee HW, Suk K, Kim SR. Therapeutic effects of human mesenchymal stem cells in a mouse model of cerebellar ataxia with neuroinflammation. J Clin Med. 2020;9:3654.
18. Park N, Sharma C, Jung UJ, Kim S, Nam Y, Kim KS, Suk K, Lee HW, Kim SR. Mesenchymal stem cell transplantation ameliorates ara-c-induced motor deficits in a mouse model of cerebellar ataxia. J Clin Med. 2023;12:1756.
19. Shibanuma M, Mashimo J, Mita A, Kuroki T, Nose K. Cloning from a mouse osteoblastic cell line of a set of transforming-growth-factor-beta 1-regulated genes, one of which seems to encode a follistatin-related polypeptide. Eur J Biochem. 1993;217:13–9.

20. Chaly Y, Hostager B, Smith S, Hirsch R. Follistatin-like protein 1 and its role in inflammation and inflammatory diseases. Immunol Res. 2014;59:266–72.
21. Chaly Y, Blair HC, Smith SM, Bushnell DS, Marinov AD, Campfield BT, Hirsch R. Follistatin-like protein 1 regulates chondrocyte proliferation and chondrogenic differentiation of mesenchymal stem cells. Ann Rheum Dis. 2015;74:1467–73.
22. Cheng KY, Liu Y, Han YG, Li JK, Jia JL, Chen B, Yao ZX, Nie L, Cheng L. Follistatin-like protein 1 suppressed pro-inflammatory cytokines expression during neuroinflammation induced by lipopolysaccharide. J Mol Histol. 2017;48:63–72.
23. Shen H, Cui G, Li Y, Ye W, Sun Y, Zhang Z, Li J, Xu G, Zeng X, Zhang Y, Zhang W, Huang Z, Chen W, Shen Z. Follistatin-like 1 protects mesenchymal stem cells from hypoxic damage and enhances their therapeutic efficacy in a mouse myocardial infarction model. Stem Cell Res Ther. 2019;10:17.
24. Mudo G, Bonomo A, Di Liberto V, Frinchi M, Fuxe K, Belluardo N. The FGF-2/FGFRs neurotrophic system promotes neurogenesis in the adult brain. J Neural Transm. 2009;116:995–1005.
25. Iwasaki K, Isaacs KR, Jacobowitz DM. Brain-derived neurotrophic factor stimulates neurite outgrowth in a calretinin-enriched neuronal culture system. Int J Dev Neurosci. 1998;16:135–45.
26. Babuska V, Houdek Z, Tuma J, Purkartova Z, Tumova J, Kralickova M, Vozeh F, Cendelin J. Transplantation of embryonic cerebellar grafts improves gait parameters in ataxic lurcher mice. Cerebellum. 2015;14:632–41.
27. Yang W, Wu Y, Wang C, Liu Z, Xu M, Zheng X. FSTL1 contributes to tumor progression via attenuating apoptosis in a AKT/GSK-3beta: dependent manner in hepatocellular carcinoma. Cancer Biomark. 2017;20:75–85.
28. Li W, Zhang L, Yin X, Ai H. The effects of Follistatin on the differentiation of human bone marrow mesenchymal stem cells into neurons-like cells. Ann Clin Lab Sci. 2020;50:3–12.
29. Liu R, Yang Y, Shen J, Chen H, Zhang Q, Ba R, Wei Y, Li KC, Zhang X, Zhao C. Fstl1 is involved in the regulation of radial glial scaffold development. Mol Brain. 2015;8:53.
30. Kumari E, Xu A, Chen R, Yan Y, Yang Z, Zhang T. FSTL1-knockdown improves neural oscillation via decreasing neuronal-inflammation regulating apoptosis in Abeta(1–42) induced AD model mice. Exp Neurol. 2023;359:114231.
31. Kim JH, Han J, Seo D, Yoon JH, Yoon D, Hong J, Kim SR, Kim MS, Lee TY, Kim KS, Ko PW, Lee HW, Suk K. Characterization of mesenchymal stem cells derived from patients with cerebellar ataxia: downregulation of the anti-inflammatory secretome profile. Cells. 2020;9:212.
32. Marcelo A, Afonso IT, Afonso-Reis R, Brito DVC, Costa RG, Rosa A, Alves-Cruzeiro J, Ferreira B, Henriques C, Nobre RJ, Matos CA, de Almeida LP, Nobrega C. Autophagy in Spinocerebellar ataxia type 2, a dysregulated pathway, and a target for therapy. Cell Death Dis. 2021;12:1117.
33. Liu YJ, Wang JY, Zhang XL, Jiang LL, Hu HY. Ataxin-2 sequesters Raptor into aggregates and impairs cellular mTORC1 signaling. FEBS J. 2024;291:1795–812.
34. Puccio H, Simon D, Cossee M, Criqui-Filipe P, Tiziano F, Melki J, Hindelang C, Matyas R, Rustin P, Koenig M. Mouse models for Friedreich ataxia exhibit cardiomyopathy, sensory nerve defect and Fe-S enzyme deficiency followed by intramitochondrial iron deposits. Nat Genet. 2001;27:181–6.
35. Alves-Cruzeiro JM, Mendonca L, Pereira de Almeida L, Nobrega C. Motor dysfunctions and neuropathology in mouse models of spinocerebellar ataxia type 2: a comprehensive review. Front Neurosci. 2016;10:572.
36. Dominici M, Le Blanc K, Mueller I, Slaper-Cortenbach I, Marini F, Krause D, Deans R, Keating A, Prockop D, Horwitz E. Minimal criteria for defining multipotent mesenchymal stromal cells. The International Society for Cellular Therapy position statement. Cytotherapy. 2006;8:315–7.
37. Huynh DP, Del Bigio MR, Ho DH, Pulst SM. Expression of ataxin-2 in brains from normal individuals and patients with Alzheimer's disease and spinocerebellar ataxia 2. Ann Neurol. 1999;45:232–41.
38. Toru S, Murakoshi T, Ishikawa K, Saegusa H, Fujigasaki H, Uchihara T, Nagayama S, Osanai M, Mizusawa H, Tanabe T. Spinocerebellar ataxia type 6 mutation alters P-type calcium channel function. J Biol Chem. 2000;275:10893–8.
39. Weyer A, Abele M, Schmitz-Hubsch T, Schoch B, Frings M, Timmann D, Klockgether T. Reliability and validity of the scale for the assessment and rating of ataxia: a study in 64 ataxia patients. Mov Disord. 2007;22:1633–7.
40. Marmolino D, Manto M. Past, present and future therapeutics for cerebellar ataxias. Curr Neuropharmacol. 2010;8:41–61.
41. Gao R, Liu Y, Silva-Fernandes A, Fang X, Paulucci-Holthauzen A, Chatterjee A, Zhang HL, Matsuura T, Choudhary S, Ashizawa T, Koeppen AH, Maciel P, Hazra TK, Sarkar PS. Inactivation of PNKP by mutant ATXN3 triggers apoptosis by activating the DNA damage-response pathway in SCA3. PLoS Genet. 2015;11:e1004834.
42. Jayabal S, Ljungberg L, Erwes T, Cormier A, Quilez S, El Jaouhari S, Watt AJ. Rapid onset of motor deficits in a mouse model of spinocerebellar ataxia type 6 precedes late cerebellar degeneration. Neuro. 2015;2:1–18.
43. Zhang MJ, Sun JJ, Qian L, Liu Z, Zhang Z, Cao W, Li W, Xu Y. Human umbilical mesenchymal stem cells enhance the expression of neurotrophic factors and protect ataxic mice. Brain Res. 2011;1402:122–31.
44. Hong J, Yoon D, Nam Y, Seo D, Kim JH, Kim MS, Lee TY, Kim KS, Ko PW, Lee HW, Suk K, Kim SR. Lipopolysaccharide administration for a mouse model of cerebellar ataxia with neuroinflammation. Sci Rep. 2020;10:13337.
45. Guyenet SJ, Furrer SA, Damian VM, Baughan TD, La Spada AR, Garden GA. A simple composite phenotype scoring system for evaluating mouse models of cerebellar ataxia. J Vis Exp. 2010;39:1787.
46. Yerger J, Cougnoux AC, Abbott CB, Luke R, Clark TS, Cawley NX, Porter FD, Davidson CD. Phenotype assessment for neurodegenerative murine models with ataxia and application to Niemann-Pick disease, type C1. Biol Open. 2022;11:52.
47. Nam Y, Kim JH, Seo M, Kim JH, Jin M, Jeon S, Seo JW, Lee WH, Bing SJ, Jee Y, Lee WK, Park DH, Kook H, Suk K. Lipocalin-2 protein deficiency ameliorates experimental autoimmune encephalomyelitis: the pathogenic role of lipocalin-2 in the central nervous system and peripheral lymphoid tissues. J Biol Chem. 2014;289:16773–89.
48. Hamel KA, Cvetanovic M. Cerebellar regional dissection for molecular analysis. J Vis Exp. 2020;166:10–3791.
49. Klockgether T. Sporadic ataxia with adult onset: classification and diagnostic criteria. Lancet Neurol. 2010;9:94–104.
50. Velazquez-Perez L, Rodriguez-Labrada R, Canales-Ochoa N, Sanchez-Cruz G, Fernandez-Ruiz J, Montero JM, Aguilera-Rodriguez R, Diaz R, Almaguer-Mederos LE, Truitz AP. Progression markers of Spinocerebellar ataxia 2. A twenty years neurophysiological follow up study. J Neurol Sci. 2010;290:22–6.
51. Velazquez-Perez LC, Rodriguez-Labrada R, Fernandez-Ruiz J. Spinocerebellar ataxia type 2: clinicogenetic aspects, mechanistic insights, and management approaches. Front Neurol. 2017;8:472.
52. Ferro A, Sheeler C, Rosa JG, Cvetanovic M. Role of microglia in ataxias. J Mol Biol. 2019;431:1792–804.
53. Cvetanovic M, Ingram M, Orr H, Opal P. Early activation of microglia and astrocytes in mouse models of spinocerebellar ataxia type 1. Neuroscience. 2015;289:289–99.
54. Yamasaki R, Yamaguchi H, Matsushita T, Fujii T, Hiwatashi A, Kira JI. Early strong intrathecal inflammation in cerebellar type multiple system atrophy by cerebrospinal fluid cytokine/chemokine profiles: a case control study. J Neuroinflammation. 2017;14:89.
55. Gu Y, Zhang Y, Bi Y, Liu J, Tan B, Gong M, Li T, Chen J. Mesenchymal stem cells suppress neuronal apoptosis and decrease IL-10 release via the TLR2/NFkappaB pathway in rats with hypoxic-ischemic brain damage. Mol Brain. 2015;8:65.
56. Teixeira FG, Panchalingam KM, Assuncao-Silva R, Serra SC, Mendes-Pinheiro B, Patricio P, Jung S, Anjo SI, Manadas B, Pinto L, Sousa N, Behie LA, Salgado AJ. Modulation of the mesenchymal stem cell secretome using computer-controlled bioreactors: impact on neuronal cell proliferation, survival and differentiation. Sci Rep. 2016;6:27791.
57. El Ouaamari Y, Van den Bos J, Willekens B, Cools N, Wens I. Neurotrophic factors as regenerative therapy for neurodegenerative diseases: current status, challenges and future perspectives. Int J Mol Sci. 2023;24:3866.
58. Moseley TA, Zhu M, Hedrick MH. Adipose-derived stem and progenitor cells as fillers in plastic and reconstructive surgery. Plast Reconstr Surg. 2006;118:121S-128S.
59. Barski JJ, Hartmann J, Rose CR, Hoebeek F, Morl K, Noll-Hussong M, De Zeeuw CI, Konnerth A, Meyer M. Calbindin in cerebellar Purkinje cells is a critical determinant of the precision of motor coordination. J Neurosci. 2003;23:3469–77.
60. Hoxha E, Balbo I, Miniaci MC, Tempia F. Purkinje cell signaling deficits in animal models of ataxia. Front Synaptic Neurosci. 2018;10:6.

61. Ip NY, Li YP, van de Stadt I, Panayotatos N, Alderson RF, Lindsay RM. Ciliary neurotrophic factor enhances neuronal survival in embryonic rat hippocampal cultures. J Neurosci. 1991;11:3124–34.
62. Fawcett JP, Alonso-Vanegas MA, Morris SJ, Miller FD, Sadikot AF, Murphy RA. Evidence that brain-derived neurotrophic factor from presynaptic nerve terminals regulates the phenotype of calbindin-containing neurons in the lateral septum. J Neurosci. 2000;20:274–82.
63. Widmer HR, Schaller B, Meyer M, Seiler RW. Glial cell line-derived neurotrophic factor stimulates the morphological differentiation of cultured ventral mesencephalic calbindin- and calretinin-expressing neurons. Exp Neurol. 2000;164:71–81.
64. Zurn AD, Winkel L, Menoud A, Djabali K, Aebischer P. Combined effects of GDNF, BDNF, and CNTF on motoneuron differentiation in vitro. J Neurosci Res. 1996;44:133–41.
65. Sharma A, Feng L, Muresanu DF, Huang H, Menon PK, Sahib S, Ryan Tian Z, Lafuente JV, Buzoianu AD, Castellani RJ, Nozari A, Wiklund L, Sharma HS. Topical application of CNTF, GDNF and BDNF in combination attenuates blood-spinal cord barrier permeability, edema formation, hemeoxygenase-2 upregulation, and cord pathology. Prog Brain Res. 2021;266:357–76.
66. Schwartz PM, Borghesani PR, Levy RL, Pomeroy SL, Segal RA. Abnormal cerebellar development and foliation in BDNF-/- mice reveals a role for neurotrophins in CNS patterning. Neuron. 1997;19:269–81.
67. Morrison ME, Mason CA. Granule neuron regulation of Purkinje cell development: striking a balance between neurotrophin and glutamate signaling. J Neurosci. 1998;18:3563–73.
68. Carter AR, Chen C, Schwartz PM, Segal RA. Brain-derived neurotrophic factor modulates cerebellar plasticity and synaptic ultrastructure. J Neurosci. 2002;22:1316–27.
69. Kawamoto Y, Nakamura S, Matsuo A, Akiguchi I. Glial cell line-derived neurotrophic factor-like immunoreactivity in the cerebella of normal subjects and patients with multiple system atrophy. Acta Neuropathol. 2000;100:131–7.
70. Mount HT, Dean DO, Alberch J, Dreyfus CF, Black IB. Glial cell line-derived neurotrophic factor promotes the survival and morphologic differentiation of Purkinje cells. Proc Natl Acad Sci U S A. 1995;92:9092–6.
71. Sasaki H, Hogan BL. HNF-3 beta as a regulator of floor plate development. Cell. 1994;76:103–15.
72. Jones J, Jaramillo-Merchan J, Bueno C, Pastor D, Viso-Leon M, Martinez S. Mesenchymal stem cells rescue Purkinje cells and improve motor functions in a mouse model of cerebellar ataxia. Neurobiol Dis. 2010;40:415–23.
73. McComish SF, Caldwell MA. Generation of defined neural populations from pluripotent stem cells. Philos Trans R Soc Lond B Biol Sci. 2018;373:20170214.
74. Naphade S, Tshilenge KT, Ellerby LM. Modeling polyglutamine expansion diseases with induced pluripotent stem cells. Neurotherapeutics. 2019;16:979–98.
75. Larkfors L, Lindsay RM, Alderson RF. Ciliary neurotrophic factor enhances the survival of Purkinje cells in vitro. Eur J Neurosci. 1994;6:1015–25.
76. Zhang J, Li Y, Chen J, Cui Y, Lu M, Elias SB, Mitchell JB, Hammill L, Vanguri P, Chopp M. Human bone marrow stromal cell treatment improves neurological functional recovery in EAE mice. Exp Neurol. 2005;195:16–26.
77. Bao X, Wei J, Feng M, Lu S, Li G, Dou W, Ma W, Ma S, An Y, Qin C, Zhao RC, Wang R. Transplantation of human bone marrow-derived mesenchymal stem cells promotes behavioral recovery and endogenous neurogenesis after cerebral ischemia in rats. Brain Res. 2011;1367:103–13.
78. Pittenger MF, Discher DE, Peault BM, Phinney DG, Hare JM, Caplan AI. Mesenchymal stem cell perspective: cell biology to clinical progress. NPJ Regen Med. 2019;4:22.
79. Chen ZY, Chai YF, Cao L, Lu CL, He C. Glial cell line-derived neurotrophic factor enhances axonal regeneration following sciatic nerve transection in adult rats. Brain Res. 2001;902:272–6.
80. Magistri M, Khoury N, Mazza EM, Velmeshev D, Lee JK, Bicciato S, Tsoulfas P, Faghihi MA. A comparative transcriptomic analysis of astrocytes differentiation from human neural progenitor cells. Eur J Neurosci. 2016;44:2858–70.
81. Parfenova OK, Kukes VG, Grishin DV. Follistatin-like proteins: structure. Funct Biomed Importance Biomed. 2021;9:999.
82. Peters MC, Di Martino S, Boelens T, Qin J, van Mil A, Doevendans PA, Chamuleau SAJ, Sluijter JPG, Neef K. Follistatin-like 1 promotes proliferation of matured human hypoxic iPSC-cardiomyocytes and is secreted by cardiac fibroblasts. Mol Ther Methods Clin Dev. 2022;25:3–16.
83. Ouchi N, Oshima Y, Ohashi K, Higuchi A, Ikegami C, Izumiya Y, Walsh K. Follistatin-like 1, a secreted muscle protein, promotes endothelial cell function and revascularization in ischemic tissue through a nitric-oxide synthase-dependent mechanism. J Biol Chem. 2008;283:32802–11.
84. Mattiotti A, Prakash S, Barnett P, van den Hoff MJB. Follistatin-like 1 in development and human diseases. Cell Mol Life Sci. 2018;75:2339–54.
85. Ji JZ, Elyaman W, Yip HK, Lee VW, Yick LW, Hugon J, So KF. CNTF promotes survival of retinal ganglion cells after induction of ocular hypertension in rats: the possible involvement of STAT3 pathway. Eur J Neurosci. 2004;19:265–72.
86. Leaver SG, Cui Q, Plant GW, Arulpragasam A, Hisheh S, Verhaagen J, Harvey AR. AAV-mediated expression of CNTF promotes long-term survival and regeneration of adult rat retinal ganglion cells. Gene Ther. 2006;13:1328–41.
87. Li KC, Zhang FX, Li CL, Wang F, Yu MY, Zhong YQ, Zhang KH, Lu YJ, Wang Q, Ma XL, Yao JR, Wang JY, Lin LB, Han M, Zhang YQ, Kuner R, Xiao HS, Bao L, Gao X, Zhang X. Follistatin-like 1 suppresses sensory afferent transmission by activating Na+, K+-ATPase. Neuron. 2011;69:974–87.
88. Liang X, Hu Q, Li B, McBride D, Bian H, Spagnoli P, Chen D, Tang J, Zhang JH. Follistatin-like 1 attenuates apoptosis via disco-interacting protein 2 homolog A/Akt pathway after middle cerebral artery occlusion in rats. Stroke. 2014;45:3048–54.
89. Xiang S, Zhang Y, Jiang T, Ke Z, Shang Y, Ning W, Yang Z, Zhang T. Knockdown of Follistatin-like 1 disrupts synaptic transmission in hippocampus and leads to cognitive impairments. Exp Neurol. 2020;333:113412.
90. Tanaka A, Ito Y, Kawasaki H, Kitabayashi C, Nishioka R, Yamazato M, Ishizawa K, Nagai T, Hirayama M, Takahashi K, Yamamoto T, Araki N. Effects of memantine on nitric oxide production and hydroxyl radical metabolism during cerebral ischemia and reperfusion in mice. J Stroke Cerebrovasc Dis. 2018;27:1609–15.
91. Xiao X, Zhang H, Ning W, Yang Z, Wang Y, Zhang T. Knockdown of FSTL1 inhibits microglia activation and alleviates depressive-like symptoms through modulating TLR4/MyD88/NF-kappaB pathway in CUMS mice. Exp Neurol. 2022;353:114060.
92. Oh WJ, Wu CC, Kim SJ, Facchinetti V, Julien LA, Finlan M, Roux PP, Su B, Jacinto E. mTORC2 can associate with ribosomes to promote cotranslational phosphorylation and stability of nascent Akt polypeptide. EMBO J. 2010;29:3939–51.
93. Ma R, Wang M, Gao S, Zhu L, Yu L, Hu D, Zhu L, Huang W, Zhang W, Deng J, Pan J, He H, Gao Z, Xu J, Han X. miR-29a promotes the neurite outgrowth of rat neural stem cells by targeting extracellular matrix to repair brain injury. Stem Cells Dev. 2020;29:599–614.
94. Dobolyi A, Vincze C, Pal G, Lovas G. The neuroprotective functions of transforming growth factor beta proteins. Int J Mol Sci. 2012;13:8219–58.
95. Kiefer R, Streit WJ, Toyka KV, Kreutzberg GW, Hartung HP. Transforming growth factor-beta 1: a lesion-associated cytokine of the nervous system. Int J Dev Neurosci. 1995;13:331–9.
96. Lenzlinger PM, Morganti-Kossmann MC, Laurer HL, McIntosh TK. The duality of the inflammatory response to traumatic brain injury. Mol Neurobiol. 2001;24:169–81.
97. Pang L, Ye W, Che XM, Roessler BJ, Betz AL, Yang GY. Reduction of inflammatory response in the mouse brain with adenoviral-mediated transforming growth factor-ss1 expression. Stroke. 2001;32:544–52.
98. Oliveira Miranda C, Marcelo A, Silva TP, Barata J, Vasconcelos-Ferreira A, Pereira D, Nobrega C, Duarte S, Barros I, Alves J, Sereno J, Petrella LI, Castelhano J, Paiva VH, Rodrigues-Santos P, Alves V, Nunes-Correia I, Nobre RJ, Gomes C, Castelo-Branco M, Pereira de Almeida L. Repeated mesenchymal stromal cell treatment sustainably alleviates machado-joseph disease. Mol Ther. 2018;26:2131–51.

Publisher's Note

Springer Nature remains neutral with regard to jurisdictional claims in published maps and institutional affiliations.